Reprinted from JOURNAL OF THE ELECTROCHEMICAL SOCIETY
Vol. 138, No. 2, February 1991
Printed in U.S.A.

Scanning Electrochemical Microscopy

VII. Effect of Heterogeneous Electron-Transfer Rate at the Substrate on the Tip Feedback Current

David O. Wipf and Allen J. Bard*

Department of Chemistry, The University of Texas at Austin, Austin, Texas 78712

ABSTRACT

The dependence of the SECM feedback current on finite heterogeneous electron-transfer (et) kinetics at the substrate electrode was examined by experimental studies of the reduction of Fe(III) in 1M H_2SO_4 at a Pt tip over a biased glassy-carbon substrate. At the extremes of very fast and very slow et rates, the feedback current was identical to the theoretical response for conducting and insulating substrates. At intermediate et rates, the feedback response depended on the et rate and the tip insulator dimensions. These results are presented as a three-dimensional calibration surface of the feedback current as a function of rate constant and tip-to-substrate distance. At very close tip-to-substrate spacings, heterogeneous rate constants greater than 1 cm s^{-1} could be distinguished. A model of the behavior of an unbiased substrate is also presented and is used to interpret experimental feedback current results.

In this paper we examine the effect of finite heterogeneous electron-transfer (et) kinetics at a substrate material on the tip response in a scanning electrochemical microscope (SECM). We show that the SECM can be used to study the heterogeneous et rate constant, k, at a substrate and suggest several applications of such measurements. The SECM has recently been shown to have promise as a tool for the examination of solid-solution interfaces (1-6). In most previous applications an electrochemically active ultramicroelectrode tip was used to obtain images of different substrate surfaces immersed in electrolyte solutions with about micrometer resolution. It can also be used to distinguish regions of different conductivity or electrochemical activity at high resolution (5, 7-9), as well as serve as a device for high-resolution microfabrication on metallic and semiconductive surfaces (10-16). In addition to its imaging capability, the SECM is an electrochemical tool that can be used to study electrode reactions and homogeneous reactions of tip-generated species that occur in the small gap between tip and substrate. In such studies the SECM is roughly analogous to the rotating ring-disk electrode or interdigitated electrode arrays.

In the most common form of the SECM experiment, the feedback mode, the tip is used to generate, via electrolysis, a reduced or oxidized mediator species. Far from the substrate, the electrolytic current assumes the steady-state value characteristic of ultramicroelectrodes (17, 18). However, as the tip is brought close to a surface, the tip current is perturbed. This perturbation is different for an insulating and for a conducting surface. At an insulator, *i.e.*, where $k = 0$, the steady-state current will decrease because the diffusion of species to the tip is blocked. The term negative feedback is used to describe this current decrease effect. At a conductive surface, however, the reduced or oxidized mediator generated at the tip can undergo electron transfer and be restored to its original oxidation state. This regeneration of the mediator in the gap between the tip and substrate causes the current to increase. The term positive feedback is used to describe this current increase effect. Simulations for a conductive surface have only considered diffusion-limited electron transfer, *i.e.*, $k \rightarrow \infty$, at the tip and substrate (19). Even for externally unbiased substrates, the rest potential of a conductive substrate is sufficient in many cases to drive the electron-transfer rate at close to the diffusion limit (3, 4, 6, 7).

However, the behavior of the feedback current under conditions where the electron-transfer rate at the conductor surface is less than the diffusion limit (the nonreversible surface) has not been addressed. The feedback current with nonzero, but finite, k at a surface could be used to measure k and to image variations in electron-transfer activity. Alternatively, the potential of a surface or portion of a surface could be deduced from the feedback current behavior. In this paper, an empirical examination of the feedback current behavior at a nonreversible surface is made as a function of electron-transfer rate and the tip-to-substrate distance. We also consider, in some detail, the feedback current behavior on unbiased, conductive

* Electrochemical Society Fellow.

substrates and the effect of the electrode size on the observed response, as well as the possibility of extracting electron-transfer kinetics from unbiased substrates.

Experimental

Reagents.—$Fe_2(SO_4)_3 \cdot 3\ H_2O$ (Alfa Products, Danvers, Massachusetts) was recrystallized from 6*M* sulfuric acid and dried at 180°C before use. Solutions were 1*M* sulfuric acid in deionized water (Milli-Q, Millipore), 2-4 m*M* Fe(III) species (from the $Fe_2(SO_4)_3 \cdot 3\ H_2O$ compound). Solutions were sparged with argon prior to each experiment.

Electrodes.—The substrate electrode was either a 3.0 mm diam glassy carbon (BAS, W. Lafayette, Indiana) or a 1.6 mm diam platinum (BAS) disk electrode. Ultramicroelectrode tips were prepared by sealing 10 μm diam platinum wire (Goodfellow Metals, Cambridge, England) or 11 μm diam carbon fiber (Thornell Type P, grade VSB-32, Union Carbide, New York) into Pyrex tubes as previously described (4). The glass ends of the ultramicroelectrode tips were ground into a conical shape with emery paper (600 grit) so that the exposed end had a total insulator diameter of about 10-20 times the electrode radius. Both the substrate and tip electrodes were polished with 1 μm diamond polish (Buehler, Limited, Lake Bluff, Illinois) before each experimental run. No other electrode pretreatment was applied. All experiments used a Hg/Hg_2SO_4 reference electrode in 1*M* sulfuric acid (MSE, +0.412V *vs.* SCE). The auxiliary electrode was platinum gauze.

Apparatus.—A four-electrode potentiostat (RDE4, Pine Instruments Company, Grove City, Pennsylvania) was used to control the tip and substrate potentials independently. To facilitate the measurement of the small currents at the tip electrode, a home-built current preamplifier with a gain of up to 10,000 was placed in series with the tip current input. Current *vs.* time or current *vs.* potential data were digitized and stored in a personal computer using a DT-2821 A/D, D/A, and DIO board (Data Translation, Incorporated, Marlboro, Massachusetts). Tip and substrate potentials were programmed either with the D/A board or a home-built triangle-wave generator triggered by the PC.

The SECM generally followed previous designs (3, 4). The tip electrode was mounted on a three-axis translation stage that used piezoelectric inchworms and a CE-1000 controller (Burleigh Instruments, Incorporated, Fishers, New York) to affect submicrometer movements. Position, axis, and velocity control of the stage was provided by TTL signals from a CTM-05 counter-time board (Metrabyte, Taunton, Massachusetts). Each TTL pulse caused a small movement (about 15 nm). Exact control of the tip movement was possible by varying the number and frequency of the pulses. Calibration of the tip movement as a function of axis and velocity was accomplished by measuring the total distance moved after a large number of pulses.

The electrochemical cell for the SECM consisted of a Teflon cup with a threaded hole in the bottom. The insulator of the substrate electrode was threaded so that it could be screwed into the bottom of the cell. The cell was mounted such that the tip was directly above the substrate electrode. Reference and auxiliary electrodes completed the circuit.

SECM procedure.—For all of the SECM experiments, the tip current (i_T) and the tip position were recorded as the tip was scanned in a direction perpendicular to the substrate surface (z-direction) at a speed of 200 nm/s. As in previous SECM studies, the tip current was not used as part of a closed-loop control system (as is done for the scanning tunneling microscope). Rather, the z-drive piezo is calibrated and tip current-distance curves were obtained with determination of an absolute tip/substrate distance by fitting the experimental curves to a simulation for a reversible ($k \rightarrow \infty$) surface. The distance scale was made dimensionless by dividing by the tip electrode radius (a). The experimental feedback current was normalized by dividing by the steady-state current obtained when the tip was not close to the substrate ($i_{T,\infty}$).

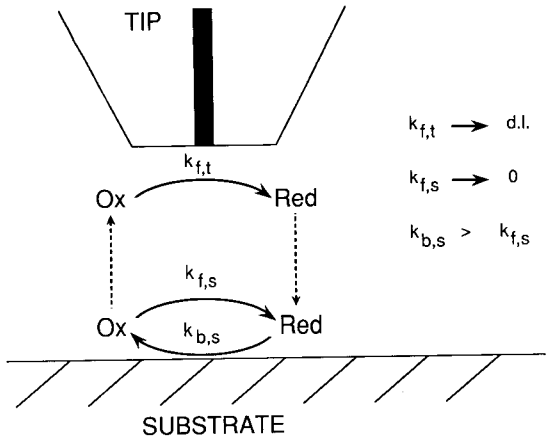

Fig. 1. Model for nonreversible electron transfer at the substrate. Solid line indicates electron transfer, d.l. means diffusion limit. Dashed line indicates diffusion.

Results and Discussion

To study the effect of a nonreversible surface on the SECM feedback mode, several experimental conditions must be maintained (Fig. 1). For a solution composed initially of the oxidized mediator, ox, the tip is set to reduce ox to red at a diffusion-limited rate. The reversible tip process is necessary for the feedback mode and implies that the potential-dependent rate constant ($k_{f,t}$) for the reduction at the tip is very large. This is readily accomplished by adjusting the tip potential, E_T, to a value that is sufficiently negative of the formal potential for the ox/red half-reaction. At the substrate, red is oxidized to regenerate ox, which diffuses into the gap between the tip and substrate and sets up the feedback condition. The rate constants for oxidation ($k_{b,s}$) and reduction ($k_{f,s}$) at the substrate are functions of the substrate potential and are given by the Butler-Volmer relations (20a)

$$k_{f,s} = k^\circ \exp[-\alpha n f(E_s - E^{\circ\prime})] \quad [1]$$

$$k_{b,s} = k^\circ \exp[(1-\alpha) n f(E_s - E^{\circ\prime})] \quad [2]$$

where k° is the standard rate constant, $E^{\circ\prime}$ is the formal potential, α is the transfer coefficient, n is the number of electrons transferred, and f is $\mathbf{F}/RT$ where $\mathbf{F}$ is the Faraday, R the gas constant, and T the temperature. The rate of feedback can, therefore, be controlled by controlling the substrate potential, E_s.

In selecting an electrode reaction to illustrate the effect of finite kinetics on the feedback current, it is convenient to choose one with a small k° value. In this case the anodic and cathodic processes are widely separated in potential so that one can examine a large range of $k_{b,s}$ values under conditions where $k_{f,s}$ remains negligibly small. Note that even if k° is small, arbitrarily large values of $k_{b,s}$ can be attained at the substrate by applying a potential sufficiently positive of $E^{\circ\prime}$ (Eq. [2]). If a half-reaction with a larger k° value is selected, only a small range of potential can be examined in the feedback mode. In this case, as E_s is moved negative with respect to $E^{\circ\prime}$, $k_{f,s}$ can become sufficiently large so that ox is reduced at both tip and substrate. This leads to depletion of ox in the gap rather than feedback, even with the tip at rather large distances from the substrate. A small value of k° is also convenient, because it allows the substrate to show essentially insulating behavior by setting E_s at a value near $E^{\circ\prime}$ where both $k_{b,s}$ and $k_{f,s}$ are negligibly small.

Fe(III)/Fe(II) kinetics.—The mediator used for the experiments reported here was the Fe(III)/Fe(II) couple in H_2SO_4. Cyclic voltammograms for the reduction of Fe(III) to Fe(II) at a glassy-carbon and a carbon-fiber electrode are shown in Fig. 2a and b. The formal potential, $E^{\circ\prime}$, was taken as −0.02V from the average value of the anodic and cathodic peak potentials. This value is the same as that found for the reduction on a platinum electrode, where the elec-

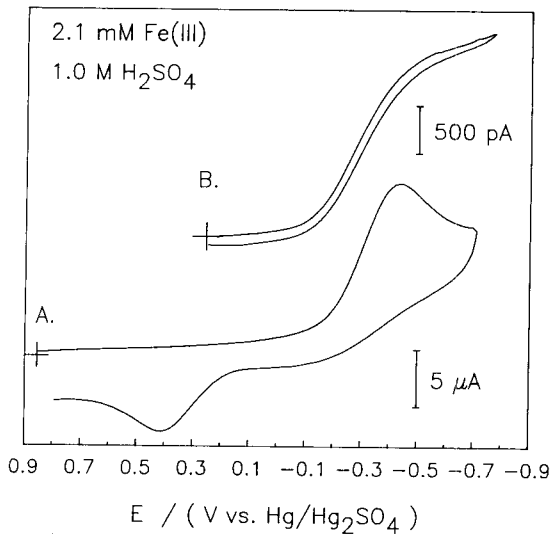

Fig. 2. Cyclic voltammograms at 50 mV s^{-1} for 2.1 mM Fe(III) in 1M H_2SO_4/water. Cross marks initial potential and zero current. (A) Voltammogram at a 3.0 mm diam glassy-carbon electrode. (B) Voltammogram at a 11 μm diam carbon-fiber electrode.

trode reaction is more reversible. An attempt was made to simulate this and other cyclic voltammetric data by a standard finite-difference calculation to obtain k° and α values. Although the peak separation was consistent with a k° of 1×10^{-6} cm s^{-1}, no combination of α or k° could exactly replicate the wave shapes. This suggests that the overall reaction at glassy carbon may involve factors other than a simple irreversible heterogeneous et reaction (*e.g.*, changes in the surface affecting k° during the scan, chemical steps, or nonuniform surface structure). However, the behavior appears sufficiently well-defined for the purposes of this study. The value of α can be assumed to be 0.5 by consideration that the averages of the peak potentials are identical at platinum and carbon electrodes. All calculations that follow used the above values for k°, α, and $E^{\circ\prime}$.

Taylor and Humffray report a standard rate constant of 1.2×10^{-3} cm s^{-1} for the reduction of Fe (III) on glassy carbon under similar conditions. However, this value was observed only after pretreatment of the GC with a chromic acid solution (21); before pretreatment, a voltammogram similar to that of Fig. 2a was observed. Numerous studies have shown that heterogeneous rate constants at GC electrodes are strongly dependent upon surface pretreatments, such as chemical and electrochemical oxidation (22). The magnitude of the transfer coefficient measured at platinum and carbon electrodes has been reported as 0.46-0.5 (21, 23-25). The k° for the Fe(III) reduction on a carbon-fiber electrode appears to be larger than that for glassy carbon. Zoski and Oldham (25) have reported an expression for the irreversible wave at a microdisk electrode. Attempts to fit the experimental data to this equation were not completely successful, but a k° of about 6×10^{-5} cm s^{-1} was indicated.

Feedback current response.—Current-distance curves for a carbon-fiber tip electrode held at −0.6V and a glassy-carbon substrate biased at 0.8 and 0.0V are shown in Fig. 3. When E_s = 0.8V, $k_{b,s}$ is very large and the response can be fit to a simulation for a reversible conductive substrate (19) (Fig. 3). When E_s = 0.0V, both $k_{f,s}$ and $k_{b,s}$ are small; the experimental response then matches the simulation for an insulator. These results illustrate how the feedback response is a function of the electron-transfer kinetics of the mediator/substrate, which can be controlled by the choice of E_s. The fitting of these data based on the ideal models allows calibration of the tip/substrate distance.

A family of feedback curves are seen if the response is recorded for a range of substrate potentials. Figure 4a shows the curves obtained for 25 mV increments in E_s between 0.8 and 0.0V. For clarity, the logarithm of the current is shown. The small regular deviations (bumps) in the

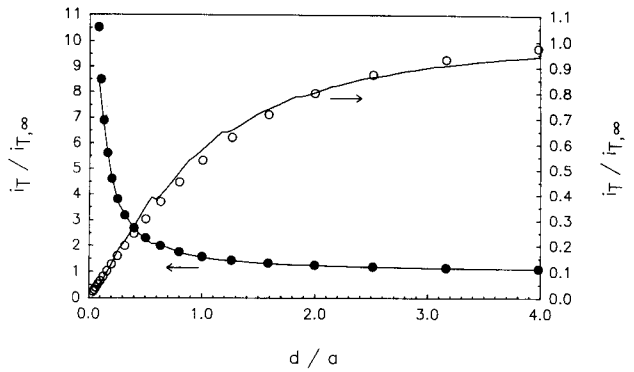

Fig. 3. SECM current-distance curves and simulation for a 2.1 mM Fe(III) solution in 1M H_2SO_4/water, note different scales. Tip electrode is 11 μm carbon fiber; substrate electrode is glassy-carbon. Solid lines are experimental data: left-substrate potential is 0.8V, tip potential is −0.6V; right-substrate potential is 0.0V, tip potential is −0.6V; (●●●) simulation for a conductor; (○○○) simulation for an insulator (insulator-to-electrode diameter of 10).

smooth response at about 0.6 d/a units are caused by the clamping action of the piezo positioner in the inchworms. Similar bumps are seen in Fig. 3. An interesting set of curves are recorded for potentials near 0.5V (Fig. 4b). Here, as the tip is moved closer to the electrode, the current increases and then decays, giving rise to a peak-shaped response. The data in Fig. 4a can be replotted as a function of distance and $k_{b,s}$ to give a 3-dimensional surface. Two views of this surface are given in Fig. 5. In this figure, conversion of the substrate potential to $k_{b,s}$ was accomplished by Eq. [2], with the assumed values of k°, α, and $E^{\circ\prime}$ indicated above.

Quantitative simulations of the general feedback current response are not yet available; however, the response can be explained qualitatively by considering the curves as a combination (not necessarily a linear one) of the reversible conductor and insulator responses. Accordingly, the response approaches that of the conductor case at more positive potentials and that of the insulator at more negative ones. This also implies that the general feedback response is affected by the tip construction, since the feedback response at an insulating substrate is strongly dependent on the ratio of the electrode insulator diameter to the electrode diameter (RG) (19). This effect is seen in Fig. 6, where

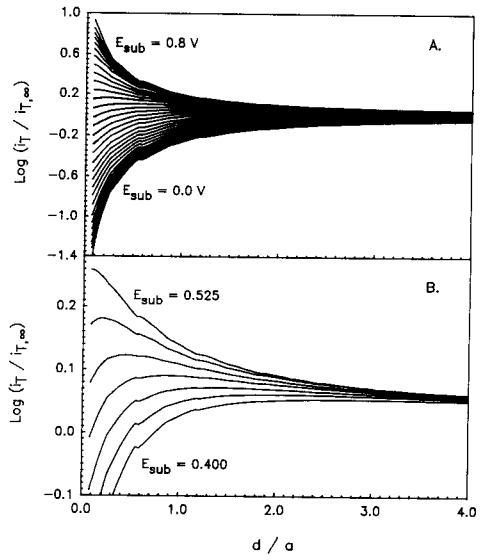

Fig. 4. SECM log current-distance curves for a 2.1 mM Fe(III) solution in 1M H_2SO_4/water. Tip electrode is 11 μm carbon fiber at a potential of −0.6V; substrate electrode is glassy-carbon. (A) Curves for different substrate potentials at 25 mV increments between 0.8 and 0.0V. (B) Region of Fig. A between 0.525 and 0.400V.

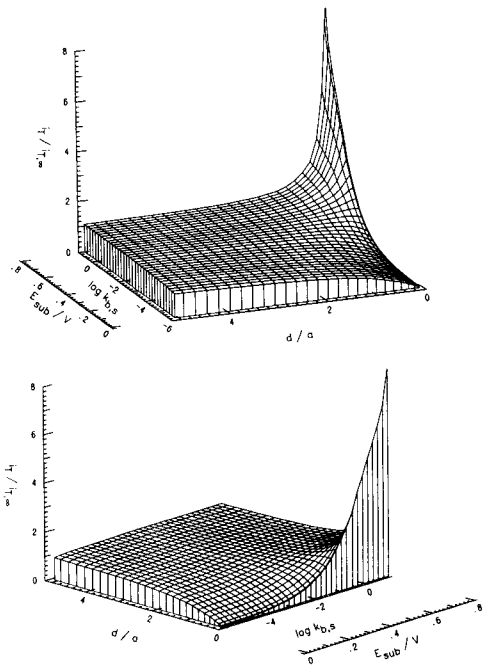

Fig. 5. Two views of the feedback current *vs.* *d/a* and log $k_{b,s}$ surface. $k_{b,s}$ calculated from E_s from Eq. [2] with $E^{o\prime} = -0.02$V *vs.* MSE, $k^o = 10^{-6}$ cm s^{-1}, and $\alpha = 0.5$.

the feedback current response is compared for two tips with the same electrode area, with ratios of insulator-to-electrode diameter of about 10 and 20. These show the greatest difference in current at more negative potentials and at closer distances. The peak-shaped response found at intermediate potentials is a result of the intermixing of insulator and conductor behavior.

At very close tip-to-substrate distances ($d/a < 0.1$), most of the current at the tip arises from the mediator species being regenerated at the substrate. Therefore, the tip current should be proportional to $k_{b,s}$ and the current density at the substrate. This is illustrated in Fig. 7, where the tip was placed at a distance of about 0.5 μm from the substrate and the feedback current was recorded as the substrate electrode potential was scanned from 0 to 0.8V and back. The log current *vs.* log $k_{b,s}$ graph from these data is linear over a wide range (about three orders of magnitude of $k_{b,s}$), up to a $k_{b,s}$ of about 0.6 cm s^{-1}. The small hysteresis at the largest rate constants is in the transition region between control of the current by the et rate and the diffusion rate. This Tafel-like plot is interesting in that very large rate constants can be determined. The effective mass-transfer coefficient, m_o, at an ultramicroelectrode is usually of the

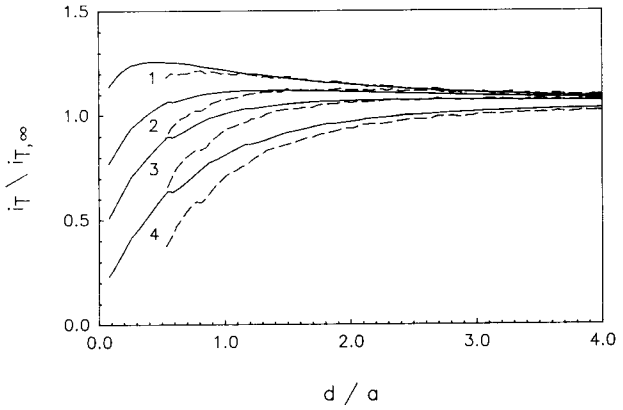

Fig. 6. Experimental feedback response for: (---) a tip with an insulator-electrode diameter ratio of 20; (——) a tip with ratio 10. Value of $k_{b,s}$: (1) 2.5 × 10^{-2}, (2) 9.4 × 10^{-3}, (3) 3.5 × 10^{-3}, and (4) 3.4 × 10^{-4} cm s^{-1}.

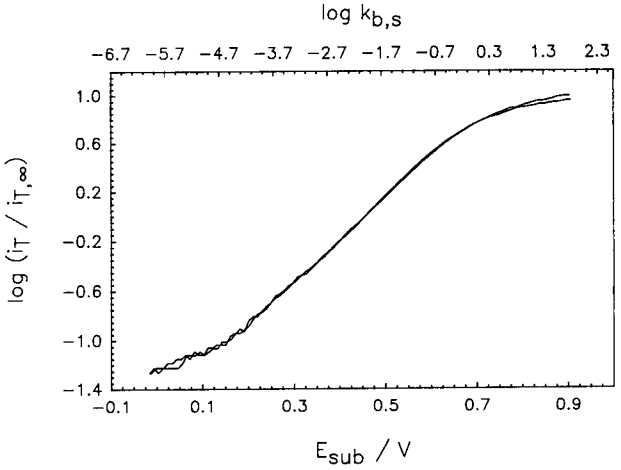

Fig. 7. Log feedback current *vs.* log $k_{b,s}$ and substrate potential, E_s, at a close tip-substrate spacing (d = 0.5 μm, d/a = 0.09), for a sweep of E_s from 0.9 to 0.0V and then back to 0.9V (sweep rate 3 mV s^{-1}).

order of D_o/a (17, 18), as expected from the steady-state current for spherical diffusion (20b). In the SECM, however, the current at the tip is increased above this steady-state value at small d by positive feedback from the substrate. Under these conditions, m_o is expected to be of the order of D_o/d. For this experiment, D_o is about 4 × 10^{-6} cm^2 s^{-1} (24) and d is 0.5 μm; therefore m_o is about 0.08 cm s^{-1}. This can be compared to a rotating disk electrode, where m_o is given by (20c)

$$m_o = 0.620\, D_o^{2/3}\omega^{1/2}\nu^{-1/6} \quad [3]$$

If the kinematic viscosity, ν, is taken as 0.01 cm^2 s^{-1}, then a rotation rate, ω, of 20,000 s^{-1} or 200,000 rpm would be required to match the mass-transfer rate in Fig. 7. This analysis suggests that the SECM should be useful for measuring very large heterogeneous rate constants by making measurements at very small d (even with electrodes of larger radii, a).

Unbiased substrate.—In previous studies of conductive substrates with the SECM we showed that a positive feedback response can be obtained even if the substrate is not connected to any external applied voltage (an unbiased substrate). This positive feedback arises when a significant area of the substrate away from the tip is bathed in a solution whose concentrations have not been perturbed by the tip reaction. However, as we demonstrate below, the feedback response at an unbiased substrate can also be per-

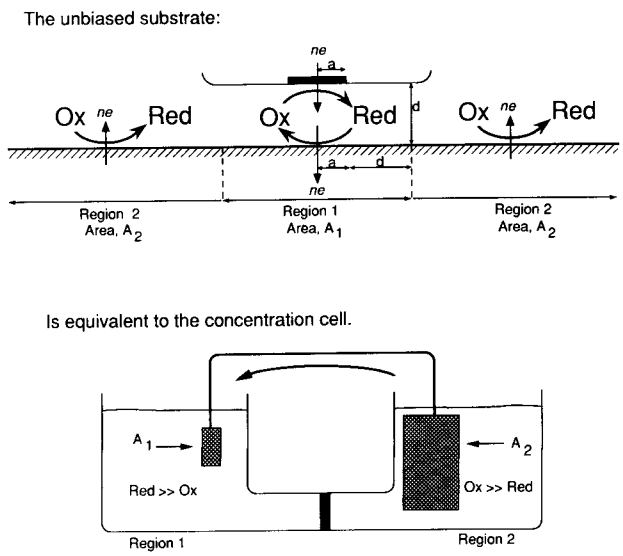

Fig. 8. Schematic illustration of an unbiased substrate

turbed by finite heterogeneous electron-transfer kinetics. For an unbiased substrate, the potential of the substrate is poised by the relative concentrations of the oxidized and reduced mediator. However, the substrate potential will be perturbed by the current flow that is required to recycle the mediator.

A description of the unbiased substrate response can be obtained by assuming that it behaves like a concentration cell (Fig. 8). The model makes the assumption that the substrate surface can be divided into two regions, 1 and 2. Region 1 has an area, A_1, roughly equal in area to $\pi(a + d)^2$, assuming a conical diffusion field extending from the tip to the substrate (see Fig. 8). In this region, the concentration of the reduced mediator is much larger than that of the oxidized mediator. The area of region 2, A_2, is simply the remaining area of the substrate (usually much larger than A_1), where the concentration of the oxidized mediator is much larger than that of the reduced form. These assumptions will hold when the tip is close to the substrate (*i.e.*, less than 5 d/a).

Current-potential curves for the two regions can be calculated from the current-potential relation (cf. Fig. 9) (20)

$$\frac{i}{n\mathbf{F}Ak^{\circ}C_O^{(1-\alpha)}C_R^{\alpha}} = \left(1 - \frac{i}{i_{l,c}}\right)\exp\left[-\alpha nf(E - E_{eq})\right] - \left(1 - \frac{i}{i_{l,a}}\right)\exp\left[(1 - \alpha)nf(E - E_{eq})\right] \quad [4]$$

where E_{eq} is the rest potential and $A = A_1$ or A_2 for regions 1 or 2, respectively. Mass-transfer effects are included by consideration of the limiting currents, which, for simplicity, are taken as

$$i_{l,c} = 4n\mathbf{F}rDC_O \quad [5]$$

$$i_{l,a} = 4n\mathbf{F}rDC_R \quad [6]$$

where r is the radius of a disk of equivalent area to A_1 or A_2. Note that these limiting currents are those expected at a finite disk electrode and may be overly conservative at the substrate, where mass transport by convection may dominate. In addition, the limiting currents in region 1 can be increased by decreasing the tip-substrate separation, thus increasing the effective mass transport by the feedback effect. When the two regions are in electrical contact, the potential of the two regions must be the same (assuming negligible ohmic drop) and a net current flows between the two regions.

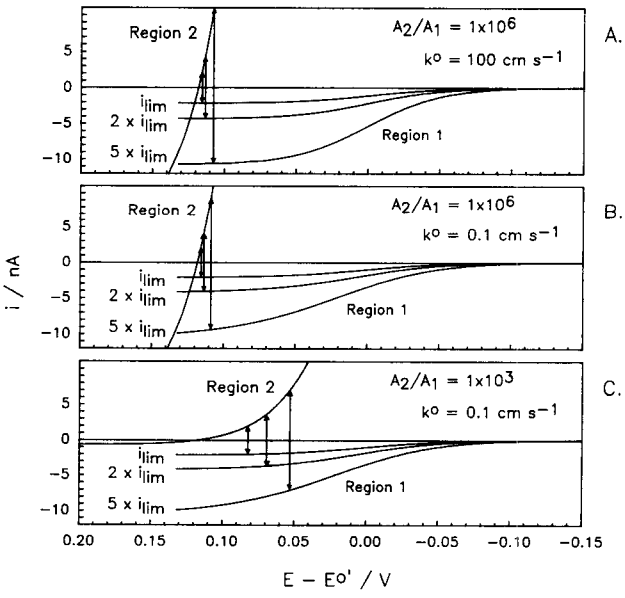

Fig. 9. Current-potential relationship for the concentration cell model (see text). Solid curves are for regions 1 and 2. The substrate curve (*i.e.*, region 2) is as labeled. The curves for region 1 are shown for 1, 2, and 5 times the limiting current, i_{lim}, expected at a finite disk. Lines with arrows indicate the potential and current values when the two regions are in electrical contact. The curves were calculated with the following values: $A_1 = 1 \times 10^{-6}$ cm^2; $\alpha = 0.5$; $T = 298$ K; $D = 1 \times 10^{-5}$ cm^2 s^{-1}; $C = 1 \times 10^{-6}$ mol cm^{-3}. The concentrations of red and ox in region 1 were taken to be 0.99C and 0.01C, respectively. Vice versa for region 2. Values for k° and A_2 are as indicated on the plots.

Figures 9a-c illustrate the behavior of the model concentration cell. At a large substrate and with a fast electron-transfer rate constant (Fig. 9a), the potential of regions 1 and 2 are only slightly more negative than the equilibrium potential of region 2. This potential is sufficient to drive the current at region 1 to the mass-transport limit. In this case, the SECM response will be essentially the response predicted by simulations for a reversible conductor. As the limiting current in region 1 increases (*i.e.*, the tip-substrate distance is decreased) the potential of the substrate must shift more negative to supply the additional current. At a large substrate, but with a slower rate constant (Fig. 9b), the current-potential curves of region 1 become quasi-reversible. The current in region 2 still approaches that of a Nernstian system, since the current density at these potentials is small. But, as the limiting current in region 1 is increased, the potential may no longer be sufficient to drive it to the mass-transport limit. In this case, the SECM response will be similar to that found for nonreversible behavior at the biased substrate (cf. Fig. 4). The most complicated behavior occurs when A_2 is small, *i.e.*, larger than A_1 by a factor of only 1000 or less. Here (Fig. 9c), the shift in potential from the equilibrium potential is large and the current at region 1 is governed by the kinetics of region 2 and the substrate potential. Thus, finite et kinetics will be important in determining the response of an unbiased conductive substrate. The deviation from the behavior expected for a substrate biased at a potential for a mass-transfer limited oxidation will become larger as k° and the area of the substrate decrease. Indeed, for unbiased conductive substrates with areas of the order of the tip area, no steady-state positive feedback current will be produced, even if k° is large.

Measurement of surface potentials.—As shown above, the positive feedback current at an unbiased substrate is a function of the potential the substrate assumes as a result of the partial currents in regions 1 and 2. Thus, the SECM can monitor the potential of an unbiased substrate by measuring the feedback current. This approach is most straightforward, as discussed above, when the substrate is much larger than the tip. We demonstrate this application of the SECM by showing how the potential of a glassy carbon substrate relaxes from an imposed value to the steady-potential. This was accomplished by recording the current-distance curves at the GC substrate electrode after the GC substrate was first brought to a potential of 0.9V and then placed at open circuit. In this experiment, the tip, held at −0.6V, was moved toward the substrate and i_T *vs.* d curves were recorded at several different times. Since the solution initially contained essentially all of the iron in the 3+ state, bringing the substrate electrode to +0.9V basically charged the substrate double layer to this potential. The substrate could relax to the more negative solution potential through oxidation of solution species, *i.e.*, tip-generated Fe(II). The initial curve (recorded 2.5 min after open circuit) shows a slight positive feedback, but curves taken after this (every 2.5 min) show an increasing negative feedback (Fig. 10). This indicates that the substrate potential is slowly decaying from 0.9V to a more negative rest potential. The potential of the unbiased substrate electrode at any time can be assigned by comparing these curves to the nearly identical curves obtained at a biased electrode (Fig. 4).

Conclusions

The tip current for the SECM operating in the feedback mode has been examined for a surface/mediator combination that does not exhibit reversible behavior. An externally biased glassy carbon substrate electrode immersed in a Fe(III) solution allowed a wide range of heterogeneous et rate constants to be studied. Moreover, the high effec-

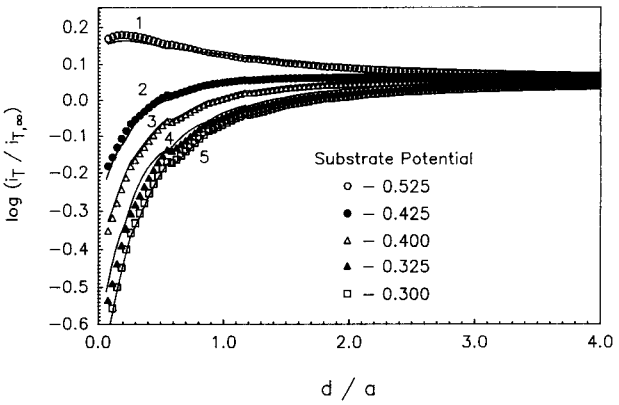

Fig. 10. SECM log current-distance curves for a 2.1 mM Fe(III) solution in 1M H_2SO_4/water. Tip electrode is an 11 μm carbon fiber at a potential of −0.6V; substrate electrode is glassy carbon that had been potentiostated at +0.9V and then brought to open circuit. Solid lines indicate the feedback response at the unbiased substrate at times of (1) 2.5; (2) 5.0; (3) 7.5; (4) 10.0; and (5) 12.5 min after the substrate was disconnected from potentiostatic control of +0.9V. Symbols represent data taken for the substrate under potentiostatic control at the potentials indicated.

tive mass-transfer coefficients available at close tip-substrate spacings allow extremely rapid heterogeneous rate constants to be determined. In addition to the heterogeneous rate constant, the feedback current response is influenced by the tip insulator to electrode diameter ratio. In the absence of digital simulations of the finite et rate effects, the experimentally determined current *vs.* distance and *vs.* rate constant curves should allow the feedback current to be used to characterize an unknown surface for variations in electrochemical activity or potential. The feedback current response of an unbiased substrate was also examined for dependence on heterogeneous et rate constant and size of the examined substrate. These considerations allow the determination of surface potentials or rate constants on unbiased substrates under certain conditions. The calibration curves presented here should also be useful in estimating electron-transfer rates of tip-generated species on a nonelectrochemical substrate (*e.g.*, a biological material).

Acknowledgment

The support of this research by The Robert A. Welch Foundation and the Texas Advanced Research Program is gratefully acknowledged. Helpful discussions with Dr. Guy Denuault are gratefully acknowledged.

Manuscript submitted July 6, 1990; revised manuscript received Sept. 17, 1990.

The University of Texas at Austin assisted in meeting the publication costs of this article.

REFERENCES

1. A. J. Bard, G. Denuault, C. Lee, D. Mandler, and D. O. Wipf, *Acc. Chem. Res.*, **23,** 357 (1990).
2. R. C. Engstrom and C. M. Pharr, *Anal. Chem.*, **61,** 1099A (1989).
3. A. J. Bard, F.-R. F. Fan, J. Kwak, and O. Lev, *Anal. Chem.*, **61,** 132 (1989).
4. J. Kwak and A. J. Bard, *Anal. Chem.*, **61,** 1794 (1989).
5. C. Lee, J. Kwak, and A. J. Bard, *Proc. Natl. Acad. Sci. USA*, **87,** 1740 (1990).
6. D. Mandler and A. J. Bard, *Langmuir*, **6,** 1489 (1990).
7. J. Kwak, C. Lee, and A. J. Bard, *This Journal*, **137,** 1481 (1990).
8. C. Lee and A. J. Bard, *Anal. Chem.*, **62,** 1906 (1990).
9. R. C. Engstrom, M. Weber, D. J. Wunder, R. Burgess, and S. Winquist, *Anal. Chem.*, **58,** 844 (1986).
10. D. H. Craston, C. W. Lin, and A. J. Bard, *This Journal*, **135,** 785 (1988).
11. O. E. Hüsser, D. H. Craston, and A. J. Bard, *J. Vac. Sci. Technol. B*, **6,** 1873 (1988).
12. O. E. Hüsser, D. H. Craston, and A. J. Bard, *This Journal*, **136,** 3222 (1989).
13. Y.-M. Wuu, F.-R. F. Fan, and A. J. Bard, *ibid.*, **136,** 885 (1989).
14. D. Mandler and A. J. Bard, *ibid.*, **137,** 1079 (1990).
15. D. Mandler and A. J. Bard, *ibid.*, **136,** 3143 (1989).
16. D. Mandler and A. J. Bard, *ibid.*, **137,** 2468 (1990).
17. R. M. Wightman and D. O. Wipf, in "Electroanalytical Chemistry," A. J. Bard, Editor, Vol. 15, p. 267, Marcel Dekker, New York (1989).
18. M. Fleischmann, S. Pons, D. Rolison, and P. P. Schmidt, "Ultramicroelectrodes," Datatech Systems, Morgantown, NC (1987).
19. J. Kwak and A. J. Bard, *Anal. Chem.*, **61,** 1221 (1989).
20. A. J. Bard and L. R. Faulkner, "Electrochemical Methods," Wiley, New York (1980), (a) pp. 95-110; (b) p. 145; (c) p. 288.
21. R. J. Taylor and A. A. Humffray, *J. Electroanal. Chem.*, **42,** 347 (1973).
22. R. McCreery, in "Electroanalytical Chemistry," Vol. 17, A. J. Bard, Editor, Marcel Dekker, New York (in press).
23. D. H. Angell and T. Dickinson, *J. Electroanal. Chem.*, **35,** 55 (1972).
24. Z. Galus and R. N. Adams, *J. Phys. Chem.*, **67,** 866 (1963).
25. C. G. Zoski and K. B. Oldham, *J. Electroanal. Chem.*, **256,** 11 (1988).